A taper tension profile maker in a converting machine

Chang Woo Lee[1], Jang Won Lee[1], Kee Hyun Shin[1,*] and Soon Oh Kwon[2]

[1]*Department of Mechanical and Aerospace Engineering, Konkuk University,
1 Hwayang-Dong, Gwangjin-Gu, Seoul 143-701, Korea*
[2]*Research center of Sung-An Machinery Ansan City, Gyunggi province, Korea*

___

Abstract

Winding is an integral operation in almost every web handling process, and a center-wound roll is one of the suitable and general schemes in a winding system. However, improper internal stresses within a center-wound roll can cause damage such as buckling, spoking, cinching, etc. Wound roll quality and performance are known to be related to the distribution of in-roll stresses. It is therefore necessary to analyze the relationship between taper tension in the winding section and internal stress distribution within the center-wound roll to prevent winding failure. But it is hard to compensate for an undesirable winding roll shape such as starring, buckling, and telescoping. This is because the winding section is the final process in a roll to roll system and has no feedback control system to correct winding roll shape directly. A time varying tension profile and accurate control of it in a winding section is one way to shape the fail-safe in-roll stress distribution of a winding roll. In this study, a new taper tension profile making method is aimed for designing high quality wound rolls. A new method to determine the proper taper tension profile was designed by analyzing the winding mechanism which includes the stress model in center-wound rolls, nip induced tension model, relationship between taper tension profile and telescoping, relationship between taper tension type and internal stress distribution. An auto taper tension profile making method was proposed not only to optimize radial stress distribution but also to minimize lateral error (telescoping). Simulation results show that the proposed method is very useful for determining the desirable taper tension profile during the winding process and preventing defects of winding roll shape such as telescoping, starting, and dishing and so on.

Keywords: Center-wound roll; CMD (Cross Machine Direction); NIT (Nip Induced Tension); Starring, Taper tension profile; Telescoping; Winding process

___

1. Introduction

Web handling is a manufacturing process which pervades almost every manufacturing industry. Winding is an integral operation and the final process in most web handling systems. Centre wound roll form is one of the most efficient and convenient storage formats for a high speed winding process. However, the internal stresses within centre wound rolls can cause damage such as buckling, spoking, cinching, etc. It is therefore essential to wind just enough stress into a wound roll so that a stable package is wound without inordinate or insufficient stress.

Early work by Altmann [1] provided a general solution of a linear elastic roll material while using a nonlinear constitutive relation to find the radial and hoop stresses for successive wraps. He solved a second order differential equation for the linear elastic material in a centre wound roll.

Yagoda established core compliance as an inner boundary condition on centre wound rolls [2]. Hakiel incorporated nonlinear material properties into the basic mechanics and numerical solutions of wound roll stresses [3].

Good et al. [4] compared results of Hakiel's model

with interlayer pressure measured by using pull tabs. They noted that the predicted stresses were twice as large as the measured values. However, they were able to bring predicted and measured values into better agreement by modifying the outer hoop-stress boundary condition to relax relative to the out-layer tensile stresses by their model of "wound on tension" loss.

Burns [5] derived a strain-based formula for stresses in profiled centre wound rolls by using residual stress model. They noted that radial stress within a wound roll is closely related to the variation of effective radial stress.

It is clear from reviewing the literature that a momentous factor for making high quality wound rolls is the taper tension profile in the winding process. Previous studies on the taper tension profile were focused on optimal radial stress distribution to minimize starring, buckling, etc. However, there is another major problem in wound rolls. That is lateral error (telescoping) in a wound roll. As the operating speed increases, the telescoping problem happens easily and seriously because the operating conditions of high speed and low tension make it easy to cause lateral instability of a moving web [6]. Winding tension is decreased according to a winding roll diameter under constant operating speed, which is called taper tension in general. In this paper, the effect of conventional taper tension profiles (linear and hyperbolic type) on radial stress distribution and telescoping which is the result of the lateral instability of the web due to tension variation was analyzed. An auto taper tension profile making method not only for optimizing radial stress distribution but also for minimizing lateral error (telescoping) was proposed. Numerical simulation results show that the proposed method is very useful to determine the desirable taper tension profile during the winding process and to prevent defects of winding roll shape such as telescoping, starring, and dishing and so on.

2. Mathematical models

2.1 Taper tension model in winding process

Fig. 1 is a schematic geometry of the tension T acting on the web and wound roll. a is core radius, R is current radius of the wound roll, M is torque, and σ_w is a taper tension profile.

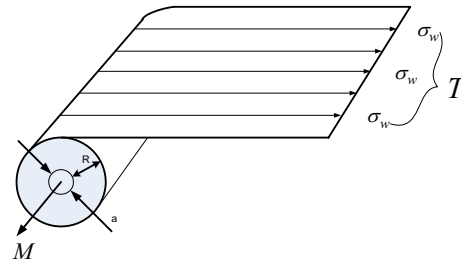In a general way, a linear and hyperbolic taper ten-
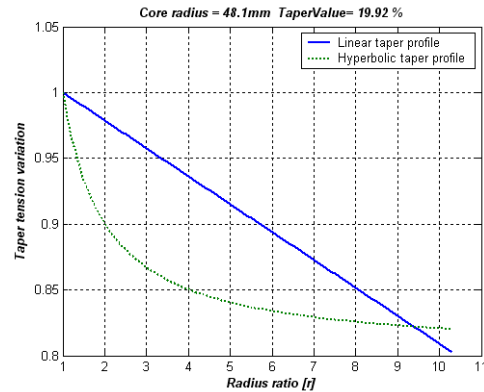

Fig. 1. Schematic of a centre wound roll.

Fig. 2. Linear and hyperbolic taper tension profile.

sion profile is applied to a winding process [3, 4]. Those can be represented as the following Eqns (1) and (2). σ_0 is initial web stress, *taper* is the decrement of a taper tension, and r is a dimensionless roll radius ratio, i.e., the wound roll radius R divided by the core radius a.

$$\sigma_w(r) = \sigma_0 \left[1 - \left(\frac{taper}{100} \right) \frac{(r-1)}{(R-1)} \right] \tag{1}$$

$$\sigma_w(r) = \sigma_0 \left[1 - \left(\frac{taper}{100} \right) \left(\frac{r-1}{r} \right) \right] \tag{2}$$

Fig. 2 shows a normalized taper tension that is the ratio of $\sigma_w(r) / \sigma_0$, for each profiles. The normalized taper tension for a hyperbolic model varies rapidly near the core and slowly near the outer layer. But it is constantly decreased for the linear taper tension model.

2.2 Nip Induced Tension (NIT)

Most of the winding is accomplished via a center winding technique in which a wound roll is directly driven by a motor and a lay-on roller is nipped on
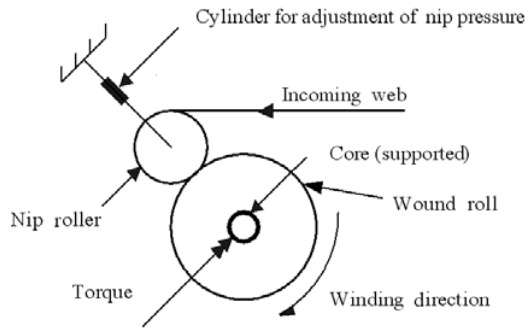
Fig. 3. A centre winder with an impinging nip roller.

Fig. 4. Effective residual stresses for two types of taper tension profile.

surface as shown in Fig. 3. The main purpose of the undriven nip roller (lay-on roller) is to help exude wound-in air from the wound roll.

Compressive force by the undriven nip roller generates an additional web tension, the nip induced tension. Total taper tension including the nip induced tension can be presented as Eq. (3) with additional term of NIT.

$$\sigma_{w\_total} = \sigma_w + NIT = \sigma_w + \frac{\mu N}{h} \quad (3)$$

where N is the nip load which may vary through the winding process, μ is the coefficient of friction between each layer of the web, and h is the web thickness.

The linear taper tension model including nipping force, Eq. (4), can be derived from Eq. (1) and Eq. (3). Substitution of Eq. (3) into Eq. (2) yields the hyperbolic taper tension model including the nipping force as shown in Eq. (5). In general, the nip load N for preventing air entrainment is set to become lower as the radius of wound roll increases.

$$\sigma_w(r) = \sigma_0\left[1 - \left(\frac{taper}{100}\right)\frac{(r-1)}{(R-1)}\right] + \frac{\mu N(r)}{h} \quad (4)$$

$$\sigma_w(r) = \sigma_0\left[1 - \left(\frac{taper}{100}\right)\left(1 - \frac{1}{r}\right)\right] + \frac{\mu N(r)}{h} \quad (5)$$

2.3 Effective Residual Stress (ERS) model within wound roll

The strains of a web are spooled onto a center wound roll lap by lap. These residual strains are part of the total strains within the roll. It creates stresses in the roll after relaxation. The mathematical model of effe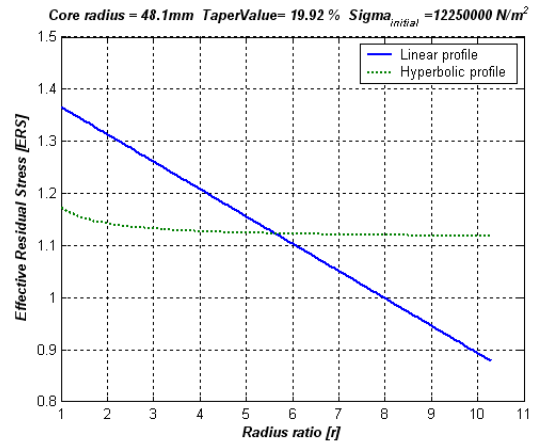ctive residual stress (ERS) is shown in Eq. (6) in which ν, σ_w means Poisson ratio of web and web stress, respectively [5].

$$\sigma^*(r) = \left(\frac{\sigma_0}{1-\nu^2}\right)\left((1+\nu)\sigma_w(r) + r\frac{d}{dr}\left(\sigma_w(r)\right)\right) \quad (6)$$

Eq. (6) shows the web stress $\sigma_w(r)$ creates the roll's residual strains. The ERS in the wound roll is from the web tension. Thus this stress depends on the roll radius ratio and on how the roll is profiled, namely, taper tension profile in rewinding section.

Eqs. (1) and (2) can be applied to Eq. (6) to derive ERS for each case of linear and hyperbolic taper tension profile. Eq. (7), follows from Eqs. (1) and (6). In the same way, the ERS for hyperbolic taper tension, Eq. (8), is derived from Eqs. (2) and (6).

$$\sigma^*(r) = \sigma_0\left(\frac{1}{1-\nu^2}\right)\left\{(1+\nu) - \left(\frac{taper}{100}\right)\left(\frac{(1+\nu)(r-1)+r}{R-1}\right)\right\} \quad (7)$$

$$\sigma^*(r) = \sigma_0\left(\frac{1}{1-\nu^2}\right)\left\{(1+\nu) - \left(\frac{taper}{100}\right)\left(\frac{r-(r-1)\nu}{r}\right)\right\} \quad (8)$$

Fig. 4 shows the ERS distribution (σ^*/σ_0) for the two taper tension profiles in which the hyperbolic taper profile has much less ERS than the linear taper profile. It means that the hyperbolic taper profile is more effective to minimize the residual strain which may induce winding quality problems (starring, buckling, etc.).

2.4 Radial stress model in wound roll

One of boundary conditions to solve the residual stress model is that the outmost layer of the wound roll is in stress free. Thus the radial stress of the wound roll is given in Eq. (9) [5].

$$\sigma_{rr}=\frac{1}{r}\left\{\left[B\left(r^{\beta}-\frac{R^{2\beta}}{r^{\beta}}\right)\right]+\frac{1}{2\beta}\left[r^{-\beta}\int_{r}^{R}t^{\beta}\sigma^{*}(t)dt-r^{\beta}\int_{r}^{R}t^{-\beta}\sigma^{*}(t)dt\right]\right\} \quad (9)$$

where

$$B=\frac{2\beta\sigma_{0}E_{c}s_{22}-\left\{\left[E_{c}\left(s_{12}-\beta s_{22}\right)-1\right]\int_{1}^{R}t^{\beta}\sigma^{*}(t)dt\right\}}{2\beta\left[\left(s_{12}E_{c}-1\right)\left(1-R^{2\beta}\right)+\right.}$$

$$\frac{-\left\{\left[E_{c}\left(s_{12}-\beta s_{22}\right)-1\right]\int_{1}^{R}t^{-\beta}\sigma^{*}(t)dt\right\}}{\left.\beta E_{c}s_{22}\left(1+R^{2\beta}\right)\right]} \quad (10)$$

and

$$\beta^{2}=\frac{s_{11}s_{33}-s_{13}^{2}}{s_{22}s_{33}-s_{23}^{2}} \quad (11)$$

In Eqs. (9) and (10), E_{c} is the hub core stiffness and s_{11}, s_{13}, s_{22}, s_{23}, s_{33} is the roll's elastic compliances.

Substitution of Eq. (7) into Eq. (9) results in Eq. (12), which means the radial stress for the linear taper tension profile. The radial stresses for the hyperbolic taper tension profile can be represented as following Eq. (13) derived from Eq. (8) and Eq. (9).

Fig. 5 shows a normalized radial stresses, $-\sigma_{rr}/\sigma_{0}$ for each taper tension profiles. On the whole, the radial stress distribution for the hyperbolic profile has equipollence more than for the linear taper profile.

$$\sigma_{rr}=\frac{1}{r}\left\{\left[B\left(r^{\beta}-\frac{R^{2\beta}}{r^{\beta}}\right)\right]+\right.$$
$$\left(\frac{1}{2\beta}\right)\left(\frac{\sigma_{0}}{1-\nu}\right)\left[\left(\frac{R^{\beta+1}-r^{\beta+1}}{\beta+1}\right)r^{-\beta}+\left(\frac{R^{1-\beta}-r^{1-\beta}}{\beta-1}\right)r^{\beta}\right]$$
$$\left.\left\{\left(\frac{2+\nu}{1+\nu}\right)\left(\frac{1}{R-1}\right)\left(\frac{taper}{100}\right)-\left[1+\left(\frac{1}{R-1}\right)\left(\frac{taper}{100}\right)\right]\right\}\right\}$$
$$(12)$$

$$\sigma_{rr}=\frac{1}{r}\left\{\left[B\left(r^{\beta}-\frac{R^{2\beta}}{r^{\beta}}\right)\right]+\right.$$
$$\frac{\sigma_{0}}{2\beta}\left\{\left(\frac{1}{1-\nu}\right)\left(1-\frac{taper}{100}\right)\left[\left(\frac{R^{\beta+1}-r^{\beta+1}}{\beta+1}\right)r^{-\beta}\right.\right.$$
$$\left.-\left(\frac{R^{1-\beta}-r^{1-\beta}}{1-\beta}\right)r^{\beta}\right]+\nu\left(\frac{1}{1-\nu^{2}}\right)\left(\frac{taper}{100}\right) \quad (13)$$
$$\left.\left(\frac{\left(\frac{R}{r}\right)^{\beta}-\left(\frac{r}{R}\right)^{\beta}-2}{\beta}\right)\right\}\right\}$$

3. Hybrid taper tension profile

3.1 Correlations between ERS and radial stress within wound roll

Fig. 6 shows the variation ($\partial\sigma_{w}/\partial r$) of the ERS for both of linear and hyperbolic taper tension profile.

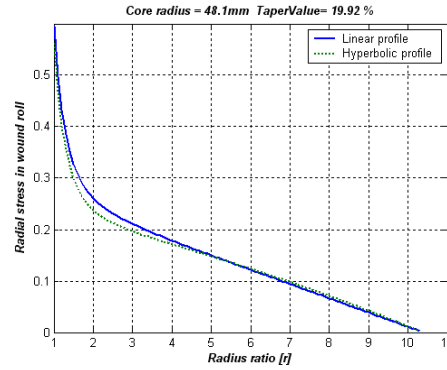In Figs. 5 and 6, a close correlation can be found

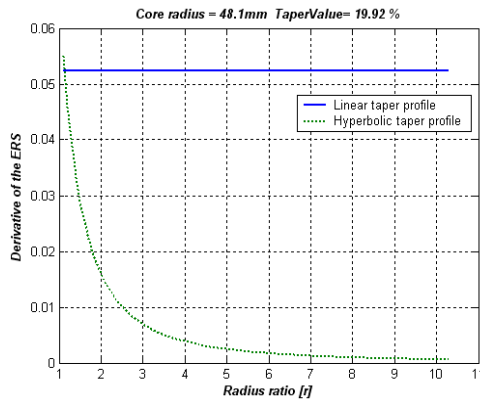Fig. 5. Radial stresses for two types of taper tension profile.

Fig. 6. Derivative of the effective residual stress.

between ERS and radial stress. As the derivative of the ERS value is low, the distribution of the radial stress becomes small and equable.

From Fig. 6, it is found that the hyperbolic taper tension profile prevents intensive increment of radial stress and promotes uniform radial stress distribution.

3.2 Relationships between taper tension profile and telescoping in the winding process

Telescoping in a wound roll can be assumed to be the result of lateral motion of a moving web during the winding process. A mathematical model of the lateral motion was derived and analyzed by considering a web of elastic beam which curves in arc or camber. Camber is the radius of curvature of a web under unforced condition lying on a flat surface. Assumed non-uniform stress distribution was applied on the cambered web as shown in Fig. 7 the induced moment is defined in Eq. (14).

$$M = r \times F = \left(\frac{W}{6}\right)(T_{max} - T_{min}) = \frac{(T_{max} - T_{min})}{6}W \tag{14}$$

From beam theory, curvature is defined as

$$\rho = \frac{EI}{M} \tag{5}$$

Substituting M of Eq. (14) into Eq. (15) leads to the curvature model of a cambered web as shown in Eq. (16)
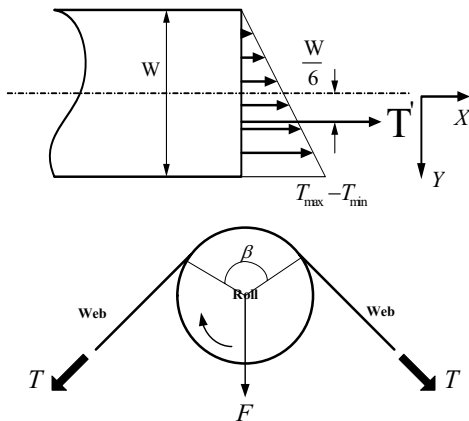
$$\rho = \frac{6EI}{(T_{max} - T_{min})W} \tag{16}$$

In Fig. 8, lateral deflection of a web at a downstream roller is shown in Eq. (17) in which L, K means length of span and stiffness coefficient [7-9].

$$y_L = \frac{2 - 2\cosh(KL) + \sinh(KL)KL}{\rho K^2 (\cosh(KL) - 1)} \tag{17}$$

The y_L in Eq. (17) is the lateral position of a moving web on a roller. It can be also considered as telescoping, because the downstream roller in Fig. 8 can be assumed to be a wound roll in the winding section.

Therefore, a mathematical model of telescoping can be derived in Eq. (18) by substituting the curvature model, Eq. (16) into the lateral deflection model, Eq. (17).

$$y_{telescoping} = \frac{2 - 2\cosh(KL) + \sinh(KL) \cdot KL}{\left[\frac{12EI}{(F_{max} - F_{min})W}\sin\left(\frac{\beta}{2}\right)\right]K^2(\cosh(KL) - 1)} \tag{18}$$

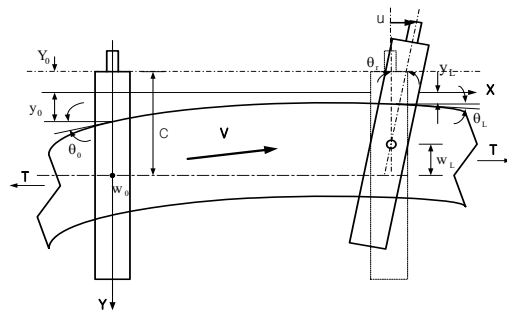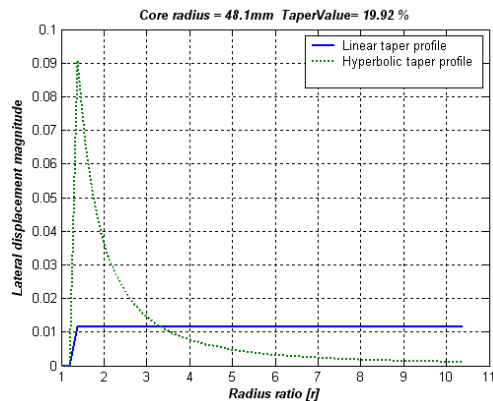Fig. 8. Boundary condition in a span.

Fig. 7. Uneven tension distribution in CMD and wrap angle.

Fig. 9. Telescoping in winding roll.

where, F is force given by web tension and β is wrap angle. The non-uniform tension distribution shown in Fig. 7 can be generated from misalignment of rollers, slippage between roller and web, non-uniform nip force, etc.

A numerical simulation study was carried out to analyze the relationships between taper tension type and telescoping phenomenon under the condition of uneven tension distribution in CMD in Fig. 7. It was found that taper tension type can affect the magnitude of telescoping, as shown in Fig. 9. It is because they have quite different tension variation according to the winding radius. It was also found that the telescoping problem could be serious at the beginning of rewinding process ($r < 2$).

3.3 Hybrid taper tension profile in winding process

Fig. 6 shows that the derivative (rate of the variation) of ERS according to wound roll radius could be lower in case of hyperbolic taper tension profile than linear taper tension profile. A lower value of the derivative of the ERS makes the radial stress distribution lower as shown in Fig. 5. These results mean that a hyperbolic tension profile is more advantageous in view of radial stress distribution.

But from Fig. 9, telescoping of wound roll near the outside of the core could be much more serious when the hyperbolic taper tension profile is applied during the winding process. The linear taper tension profile is more advantageous for preventing or minimizing the telescoping of the wound roll at the beginning of the winding process, but it could make the radial stress higher.

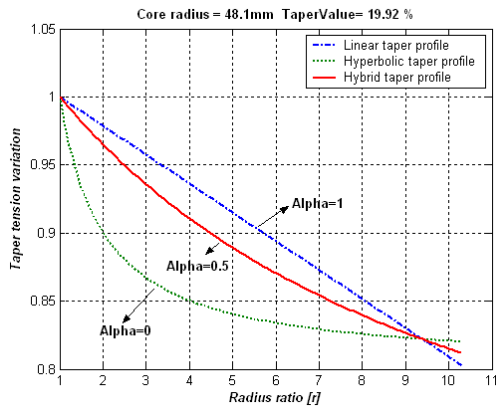A hybrid taper tension profile could be designed to

take advantage of each linear and hyperbolic taper tension profile by combining both algorithms. Eq. (19) shows the mathematical model of the newly proposed hybrid taper tension profile. The models of ERS and radial stress distribution of wound roll using the hybrid taper tension profile are Eqs. (20) and (21).

$$\sigma_w(r) = \sigma_0 \left[1 - \left(\frac{taper}{100} \right) \frac{(r-1)}{\{r + \alpha \cdot (R-r-1)\}} \right] \quad (19)$$

$$\sigma^*(r) = \left[\frac{\sigma_0}{1-v^2} \right] \left\{ (1+v) - \left(\frac{taper}{100} \right) \right.$$

$$\left. \left(\frac{(r^2 + v(r^2 - r)) + \alpha \cdot [R-r-1][(1+v)(r-1)+r] + r(r-1)]}{[r + \alpha \cdot (R-r-1)]^2} \right) \right\} \quad (20)$$

$$\sigma_{rr} = \frac{1}{r} \left\{ \left[B\left(r^\beta - \frac{R^{2\beta}}{r^\beta} \right) \right] + \left(\frac{1}{2\beta} \right) \left(\frac{\sigma_0}{1-v^2} \right) \right.$$

$$\left[\left[(\frac{1+v}{1+\beta})(\frac{R^{1+\beta}}{r^\beta} - r) - (\frac{taper}{100})r^{-\beta} \int_r^R t^\beta \left(\frac{(t^2 + v(t^2 - t))}{} \right. \right. \right.$$

$$\left. - \left[(\frac{1+v}{1-\beta})(\frac{r^\beta}{R^{1-\beta}} - r) - (\frac{taper}{100})r^\beta \int_r^R t^{-\beta} \left(\frac{(t^2 + v(t^2 - t))}{} \right. \right. \right.$$

$$\left. + \frac{\alpha \cdot [(R-t-1)[(1+v)(t-1)+t] + t(t-1)]}{[t + \alpha \cdot (R-t-1)]^2} \right) dt \right]$$

$$\left. \left. + \frac{\alpha \cdot [(R-t-1)[(1+v)(t-1)+t] + t(t-1)]}{[t + \alpha \cdot (R-t-1)]^2} \right) dt \right] \right\} \quad (21)$$

The weight factor α in Eq. (19) determines the
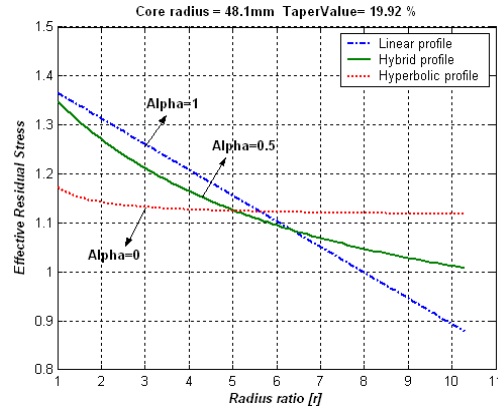

Fig. 10. Hybrid taper tension profile.

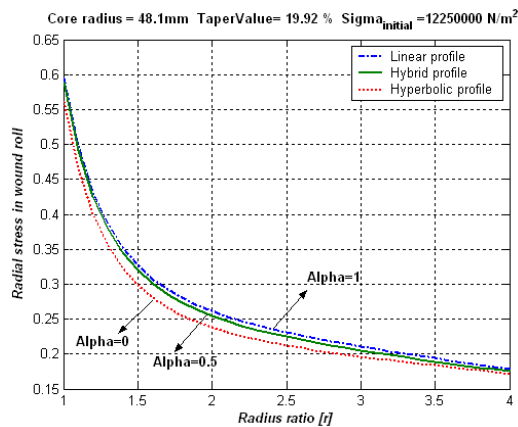Fig. 11. ERS for three taper types.

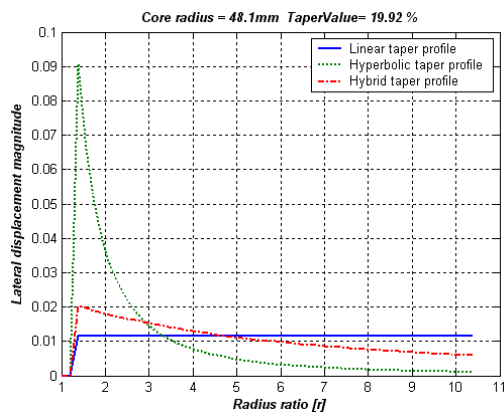Fig. 12. Radial stresses for three taper types.

Fig. 13. Induced telescoping for three taper types in rewinding roll.

contribution of both a linear and hyperbolic profile in designing a new hybrid taper tension profile. A value 1 and 0 of α means linear and hyperbolic taper tension profile of each other as shown in Fig. 10.

Fig. 11-Fig. 13 show simulation results of the ERS, radial stress distribution and induced telescoping of a wound roll when the hybrid taper tension profile was applied to a winding process.

From these simulation results, it was found that applying the hybrid taper tension profile during a winding process can reduce the magnitude of radial stress distribution and telescoping in wound rolls within satisfying a boundary.

4. Conclusion

The effect of the taper tension profile during winding process on the radial stress distribution and tele-

scoping phenomena was analyzed, which affects the wound roll quality and productivity of final product in a web handling system.

The following conclusions can be drawn from this study:

A hybrid taper tension model and telescoping model of a winding system have been developed, and the model has been verified by numeric simulation.

A relationship between taper tension profile and radial stress distribution is confirmed.

A hyperbolic taper tension profile is desirable for optimizing the radial stress of a wound roll.

A relationship between taper tension profile and telescoping is confirmed.

A linear taper tension profile is useful for minimizing the telescoping of a wound roll.

A hybrid taper tension profile generation algorithm of a winding system has been developed, and the performance has been verified by numeric simulation.

In a hybrid taper tension profile, the type of taper tension profile can be shaped according to the weighting factor (α) to minimize the telescoping ($r < 2$) and to optimize the radial stress distribution ($r > 2$).

References

[1] H. C. Altmann, Formulas for computing the stresses in center-wound rolls, *Tappi Journal* 51 (1968) 176-179.

[2] H. P. Yagoda, Resolution of a core problem in wound rolls, *Journal of Applied Mechanics* 47 (1980) 847-854.

[3] Z. Hakiel, Nonlinear model for wound roll stresses, *Tappi Journal* 70 (1987) 113-117.

[4] J. K. Good, J. D. Pfeiffer, R. M. Giachetto, Losses in wound-on-tension in the center winding of wound rolls, Proceeding of the Web Handling Symposium, ASME Applied Mechanics Division 149 (1992) 1-12.

[5] S. J. Burns, R. R. Meehan and J. C. Lambropoulos, 1999, Strain-based formulas for stresses in profiled center-wound rolls, *Tappi Journal* 82 (7) (1999) 159-167.

[6] K. H. Shin., S. O. Kwon, The effect of tension on the lateral dynamics and control of a moving web, *IEEE Trans. on Industry Applications* 43 (2005) 403-412.

[7] J. Shelton, Lateral Dynamics of a Moving Web, Ph. D. dissertation, Oklahoma state Univ. Stillwater, USA (1986).

[8] J. Shelton, K. N. Reid, Lateral dynamics of a real moving web, *ASME Journal Dynamics, Syst., Measurement, Control* 93 (1971) 180-186.

[9] J. Shelton, The effect of camber on handling, Proceeding of the international Conference on Web Handling, Oklahoma state Univ. Stillwater, USA (1997) 248-263.